

# Effect of seeded substrates on hydrothermally grown ZnO nanorods

Sunandan Baruah · Joydeep Dutta

Received: 4 January 2009 / Accepted: 5 February 2009 / Published online: 19 February 2009  
© Springer Science+Business Media, LLC 2009

**Abstract** We report a study on the effect of seeding on glass substrates with zinc oxide nanocrystallites towards the hydrothermal growth of ZnO nanorods from a zinc nitrate hexahydrate and hexamethylenetetramine solution at 95 °C. The seeding was done with pre-synthesized ZnO nanoparticles in isopropanol with diameters of about 6–7 nm as well as the direct growth of ZnO nanocrystallites on the substrates by the hydrolysis of pre-deposited zinc acetate film. The nanorods grown on ZnO nanoparticle seeds show uniform dimensions throughout the substrate but were not homogeneously aligned vertically from the substrate and appeared like nanoflowers with nanorod petals. Nanorods grown from the crystallites formed in situ on the substrates displayed wide variations in dimension depending upon the preheating and annealing conditions. Annealing the seed crystals below 350 °C led to scattered growth directions whereupon preferential orientation of the nanorods perpendicular to the substrates was observed. High surface to volume ratio which is vital for gas sensing applications can be achieved by this simple hydrothermal growth of nanorods and the rod height and rod morphology can be controlled through the growth parameters.

**Keywords** ZnO · Nanorods · Hydrothermal · Seeding · Crystallization · Sensing

## 1 Introduction

Nanostructured materials have received attention in a wide range of fields due to its interesting properties, which render them suitable for potential applications in microelectronic and optoelectronic devices [1]. Compared to bulk materials, nano-crystalline materials exhibit completely different properties due to its higher surface-to-volume ratio and also due to quantum confinement effects [2]. ZnO nanowires and nanorods are being actively studied as they are attractive candidates for a wide variety of applications such as in gas sensors [3, 4], solar cells [5], piezotronic devices [6], optoelectronics [7], etc. Different applications will entail different size and orientation of the nanorods. Gas sensors exploit the effective surface area for gas adsorption and therefore dense growth of rods is ideal for such applications. However, devices based on the piezoelectric property of the ZnO nanorods will require gaps between the rods, especially near the tips, to get sufficient deformation for generating the required voltage. All these call for a systematic study on the growth dimension and orientation of the ZnO nanorods which will facilitate the fabrication of nano devices considerably.

Numerous methods are available for the growth of ZnO nanorods, however, the most energy-efficient and economical method for synthesizing ZnO nanorods is the hydrothermal process. The hydrothermal process is an environmentally friendly process and does not require a complex vacuum environment. This process induces anisotropic crystal growth in an aqueous solution [4, 8]. The hydrothermal process is surface independent [9] and provides good control over the morphology of the nanowires grown [10]. First reported by Vayssieres et al. [8], the hydrothermal process uses an equimolar solution of zinc

S. Baruah · J. Dutta (✉)  
Center of Excellence in Nanotechnology, School of Engineering  
and Technology, Asian Institute of Technology, Pathumthani  
12120, Thailand  
e-mail: joy@ait.asia

nitrate and hexamine to epitaxially grow ZnO rods on various substrates seeded using small crystallites of ZnO. With a hexagonal wurtzite structure, the ZnO crystal exhibits fractional polar characteristics [11] with lattice parameters  $a = 0.3296$  and  $c = 0.52065$  nm. One end of the basal polar plane terminates in partially positive Zn lattice points and the other end terminates in partially negative oxygen lattice points. Sugunan et al. [10] has reported that hexamine, being a non ionic tertiary amine derivative and a nonpolar chelating agent, preferentially attaches to the nonpolar facets of the ZnO crystal, thereby exposing only the (001) plane for epitaxial growth. Thus preferential growth along the (0002) direction is possible. ZnO nanorods can be grown on a variety of substrates by affixing pre-synthesized seeds [12]. The seeding of the substrate with ZnO crystals was found to lower the thermodynamic barrier by providing nucleation sites, further improving the aspect ratio of the synthesized nanowires [8]. The seeding of the substrate is therefore an important factor in the hydrothermal growth of ZnO. Seeding can be carried out by processes such as dip coating and spin coating [12] using a colloidal solution of ZnO nanoparticles, deposition of a thin layer of ZnO particles through sputtering [13] or growing a thin crystalline film on the substrate itself.

In this work, we have compared the growth of ZnO nanorods on substrates seeded with pre synthesized and in situ grown nanoparticles of ZnO on glass substrates. Undoped ZnO are usually n-type material but doping of zinc oxide is often used to produce the defects that increase its influence on the sensors conductivity and enhance their properties with impurities, such as Sn, Cu, Al, etc. The main aim of this work was to study the effect of processing conditions on the growth of ZnO nanorods.

## 2 Experimental

### 2.1 Synthesis of ZnO nanoparticles

ZnO nanoparticles were synthesized in 2-propanol using the procedure reported by Bahnemann et al. [14] 1 mM zinc acetate [ $\text{Zn}(\text{CH}_3\text{COO})_2$ , Merck, 99% purity] solution was prepared in 20 ml of 2-propanol [ $(\text{CH}_3)_2\text{CHOH}$ , Carlo Erba, 99.7% purity] under vigorous stirring at 50 °C. The solution was then diluted to 230 ml with 2-propanol and cooled in the ambient following which 20 ml of 20 mM sodium hydroxide in 2-propanol was added dropwise to the solution under continuous stirring. The mixture was then kept in a temperature controlled water bath at 60 °C for 2 h. The transparent colloidal solution of ZnO nanoparticles was found to be stable over a period of several months.

### 2.2 Seeding on glass substrates

The substrates were first dipped in a 1% solution of dodecane thiol to self-assemble a thin layer of thiol on the silica surface [15] and thereby assist in the proper attachment of the seeds to the glass substrate. The seeding was carried out by dipping the substrate in a concentrated colloidal solution of ZnO nanoparticles using a custom-built dip coater [16] Claesson and Philipse [17] have reported that the surface functionalization of silica using thiol lead to irreversible binding of metal oxide particles from a solution. The loosely attached nanoparticles were then removed after each dipping by washing with deionised water so that particles attach properly in successive dipping. The thin film of ZnO nanocrystallites was prepared by dip coating using a 1 mM zinc acetate solution in ethanol. Preheating of the substrate was done at 100 and 120 °C and post annealing at different temperatures (100, 150, 200, 250, 350 and 450 °C) for 1 and 5 h were carried out during the experiments reported in this work.

### 2.3 Hydrothermal growth of ZnO nanorods

The ZnO nanorods were grown in a sealed chemical bath containing a 10 mM solution of zinc nitrate hexahydrate [ $\text{Zn}(\text{NO}_3)_2 \cdot 6\text{H}_2\text{O}$ , Aldrich, 99% purity] and hexamethylene tetramine ( $\text{C}_6\text{H}_{12}\text{N}_4$ , Carlo Erba, 99.5%) at 90 °C. As the growth rate considerably decreases after about 5 h, the precursor solution was changed every 5 h and growth was continued up to 15 h. The samples were then heated at 250 °C for 1 h to remove any organic deposits from the precursors.

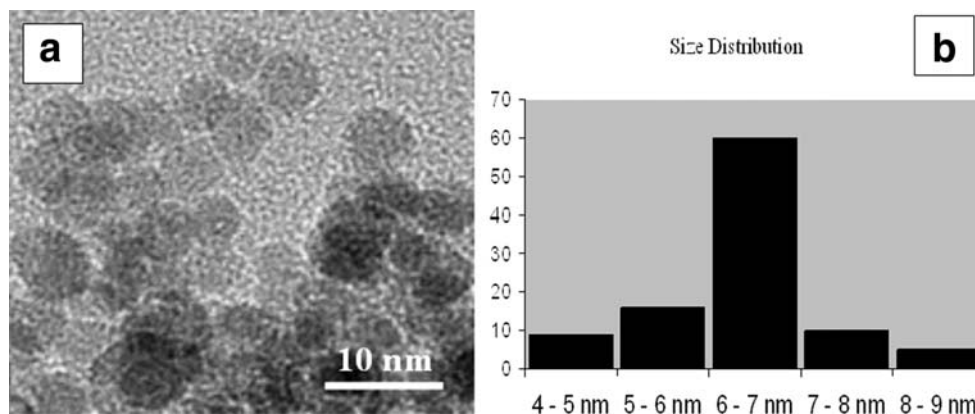
### 2.4 Characterization

Transmission electron microscopy (TEM) was done to characterize the ZnO seed nanoparticles using a JEOL/JEM 2010 TEM operated at 20 KV. Image processing software (Scion Image) was used to quantify the nanorod dimensions and density of growth on scanning electron microscope (SEM) images taken in a JEOL JSM-6301F SEM.

## 3 Results and discussion

The colloidal solution consisted of uniform ZnO nanoparticles with diameters of approximately 6–7 nm, as observed from the TEM image shown in Fig. 1a. In alcohol, the surface remains positively charged as the surface groups do not readily exchange protons with alcohol as they do with water. Acetate ions interact with the surface of zinc oxide. The (100) surface are both monodentate and

**Fig. 1** **a** Transmission electron micrograph showing the ZnO nanoparticles **b** Size distribution histogram (100 particles sampled)



tridentate oxygen coordination sites while the (001) surface is a monodentate Zn–O site. The (001) surface is characterized by  $Zn_3-O$  site that is distinct from the tridentate site found on the (100) surface due to differences in bond length. The growth rate of crystal is affected by the chemical processes of monomer addition, as well as the charge state of each facet, whereby a highly charged facet will repel ions of like charge and thereby slow the growth rate, leading to the formation of stable zinc oxide nanocrystals. The electron micrographs were analyzed to determine the particle size distribution, which shows the dominance of particles in the 6–7 nm range (Fig. 1b). The nanoparticles were synthesized in alcoholic media to avoid the formation of hydroxides since  $Zn(OH)_2$  forms more readily in water than ZnO, and as the dielectric constant of water (78.4 at 25 °C) is much higher than that of alcohol (around 18 at 25 °C), the nucleation and growth of the ZnO nanoparticles is much faster in alcohol resulting in finer well defined crystallite growth. The particles are monocrystalline with a wurtzite structure as has been reported elsewhere [18].

A SEM micrograph of the thiolated glass substrate seeded with ZnO nanoparticles is shown in Fig. 2a. It can

be observed that the ZnO nanoparticles agglomerate during the seeding process to form bigger clumps of around 30–40 nm sizes. This can be attributed to occur due to the surface tension of the solvent (ethanol) which brings the particles together during the drying process [19]. The gradual evaporation of the solvent from the surface of the substrate leads to cracks in the thin film of the nanoparticles grown on the substrates. As the particles are brought together due to surface tension of the solvent during evaporation, it is unlikely that the crystallites would be preferentially oriented on the substrate surface [20]. As a result of multifarious orientations of the seed crystallites, the nanorods grow in various directions resulting in a flower like growth. However, as the seed particles are of comparable sizes (6–7 nm), all the nanorods have similar dimensions (width  $\sim$ 400 nm) which can be observed in the SEM image shown in Fig. 2b.

To obtain highly oriented growth, seeding the substrate through direct hydrolysis on the substrate using zinc acetate appears to be a more promising technique than using pre-synthesized ZnO crystallite seeds self-organised on the substrate. Orientation of the crystallites formed in the thin film grown on the substrate depends upon the preheating as

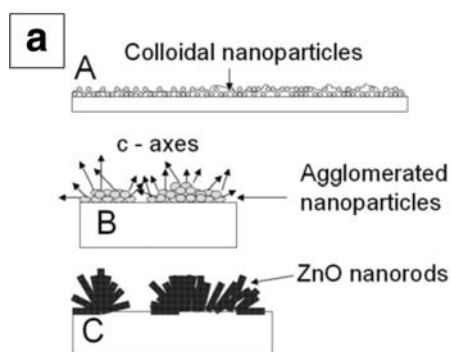
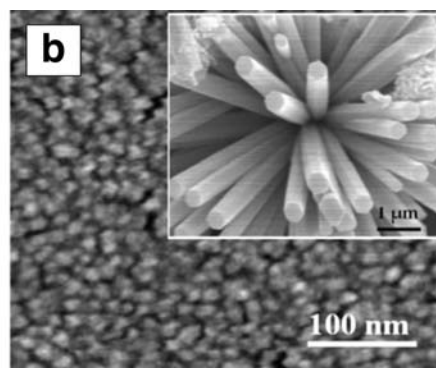
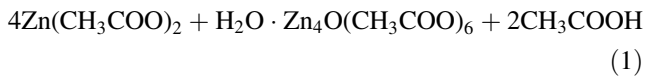


**Fig. 2** **a** Schematic diagram showing the possible agglomeration of ZnO nanoparticles upon evaporation of the solvent (A) thin layer of colloidal nanoparticles (B) agglomerated clumps of ZnO nanoparticles with various orientations of the c-axes of the nanocrystallites (C)

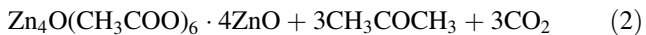


ZnO nanorods grow from the seed crystallites in the direction of the c-axes **b** Scanning electron microscope (SEM) image of ZnO particle seed layer using colloidal ZnO nanoparticles. Inset: ZnO nanorods grown using a 10 mM growth solution for 15 h

well as the post annealing temperatures [21]. Zinc acetate is known to decompose at a temperature of 237 °C [22] through the formation of basic zinc acetate arising from the loss of acetic anhydride. Acetic anhydride further hydrolyses to form acetic acid as in Eq. 1.



When the temperature of the reactant solution is increased to about 300 °C, decarboxylation occurs and basic zinc acetate decomposes to its oxide leading to the formation of ZnO nanocrystallites, as shown in Eq. 2 [23].



As zinc acetate is available in hydrated form and also the seeding solution was an aqueous solution, ZnO crystals can

start forming from zinc hydroxides at temperatures as low as 80 °C [24]. In order to study the effect of annealing of the seeded substrates on the morphology of the ZnO nanorods grown by the hydrothermal process, a series of experiments were designed wherein seeded substrates were annealed in the ambient at temperatures starting from slightly above the preheating temperature of 120 °C i.e., 150–450 °C for a period of 1 h.

Figure 3a shows the SEM image of the seed layer grown with a preheating temperature of 120 °C and post annealing at 150 °C for 1 h. Some crystals can be observed dispersed in an amorphous phase as evidenced from the diffraction pattern shown in Fig. 4b. The ZnO nanorods grown on this substrate showed wide variations in size with widths ranging from 50 nm to about 800 nm, as can be observed in the SEM image in Fig. 3b. The directions of

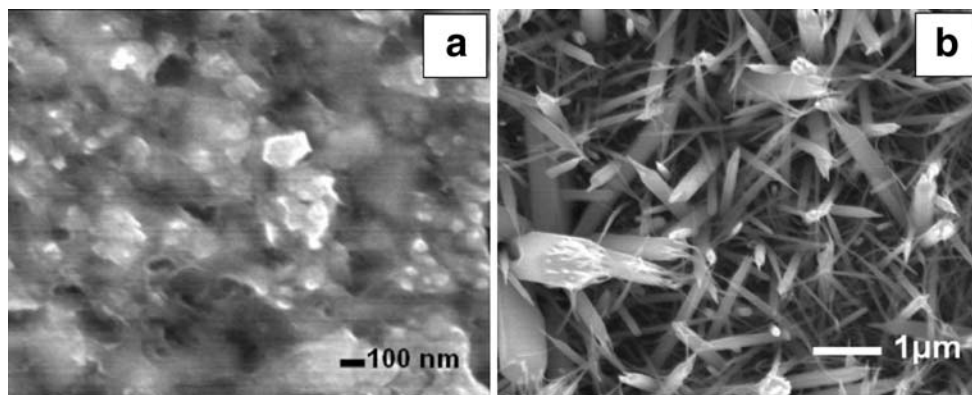


**Fig. 3** **a** Substrate seeded with zinc acetate with preheating at 120 °C and post annealing at 150 °C **b** Scanning electron microscope (SEM) image of ZnO nanorods grown on (a) using a 10 mM chemical bath

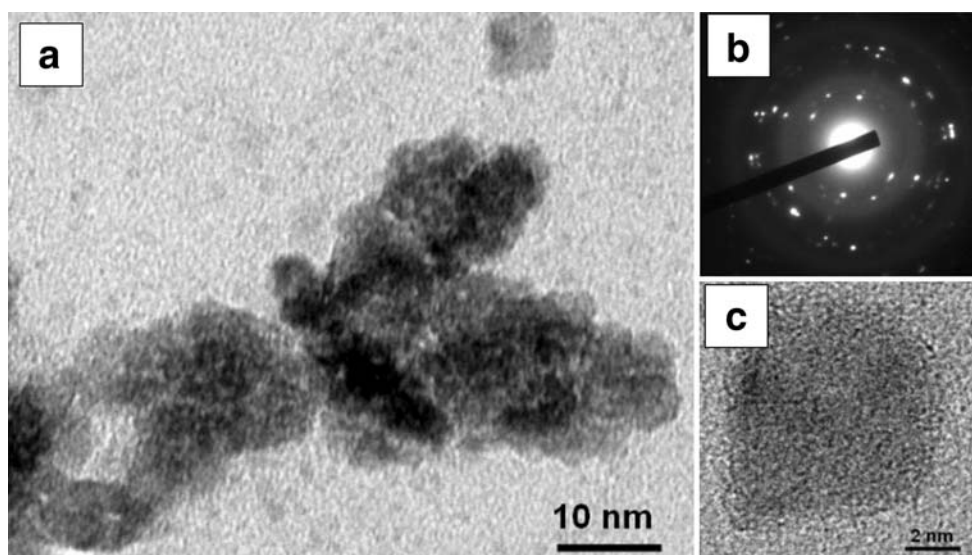


**Fig. 4** **a** Transmission electron microscope (TEM) image of the seeds formed at a preheating temperature of 120 °C and post annealing at 150 °C for 1 h **b** Diffraction pattern on the seed layer **c** HRTEM image of a single particle

growth of the rods are not specific and the nanorods appear haphazardly distributed on the substrate. Figure 4a show the TEM image of a similar film grown on a carbon coated copper grid. Even with high resolution TEM (Fig. 4c) the crystalline facets of the ZnO nanocrystallites could not be discerned.

Upon increasing the post annealing temperature to 250 °C, crystallization is enhanced with the crystallites forming 50 nm nanoparticles which also merge into larger agglomerates. The particles are clearly visible in the SEM image shown in Fig. 5a. Figure 5b show the nanorods grown from the seeded layer shown in Fig. 5a. The nanorods did not follow a specific growth direction, but compared to the previous case of post annealing at 150 °C, the size distribution of the nanorods is very narrow, with

majority of the rods grown with widths lying between 130 and 160 nm.

The diffraction pattern shown in Fig. 6b indicates the presence of single crystalline phases. Measurements done on various sections of the TEM image shown in Fig. 6a gave lattice fringe widths of 0.26, 0.28, and 0.29 nm, indicating the presence of the (002), (100), and (101) faces of the wurtzite structure of the ZnO crystal. The presence of all these faces are in conformation to the SEM image in Fig. 5b where the nanorods are observed to grow in different directions in effect not showing any preferential orientation on the substrates. To grow nanorods vertically from the substrate, the seed crystalline film should have the (002) face oriented upwards, which is the anisotropic growth direction [10, 25, 26].

**Fig. 5** **a** Substrate seeded with zinc acetate with preheating at 120 °C and post annealing at 250 °C for 1 h **b** Scanning electron microscope (SEM) image of ZnO nanorods grown on (a) using a 10 mM chemical bath

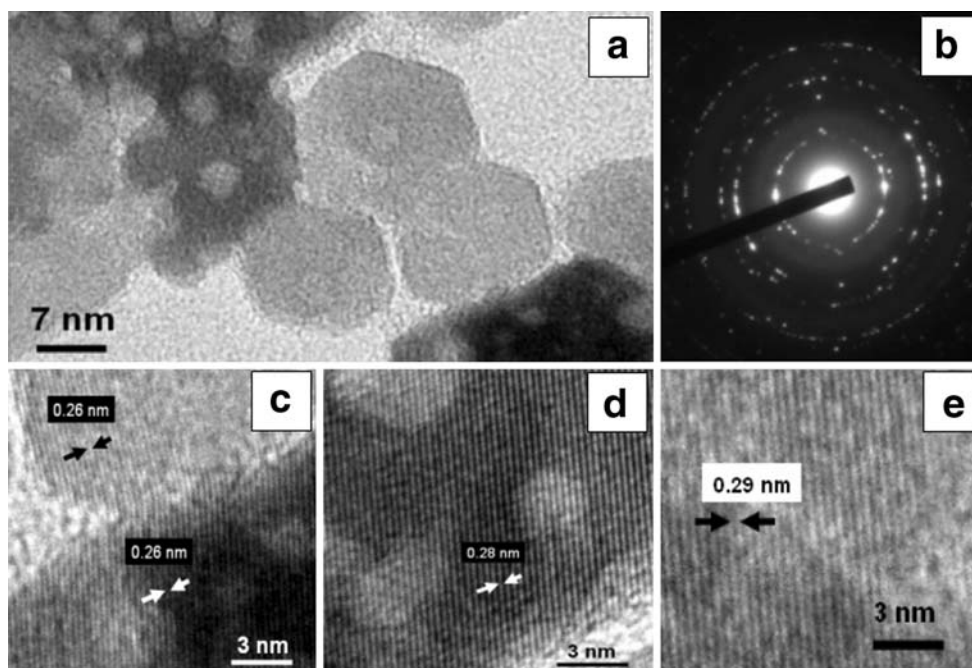
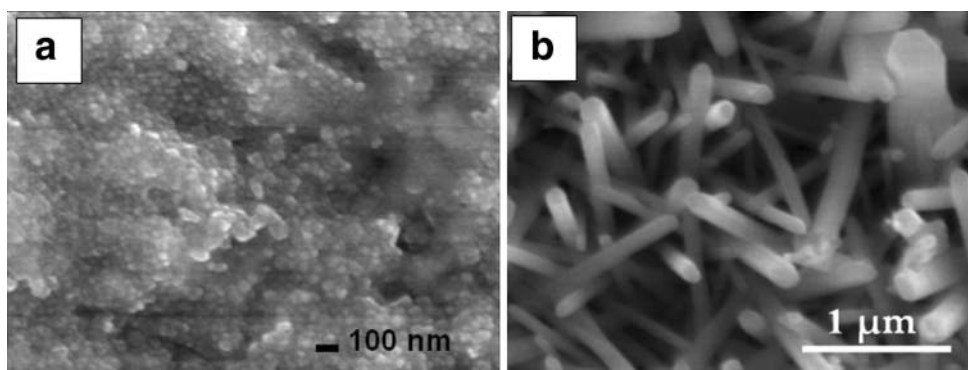


**Fig. 6** **a** Transmission electron microscope (TEM) image of the seeds formed at a preheating temperature of 120 °C and post annealing at 250 °C for 1 h **b** Diffraction pattern on the seed layer **c, d, e** Lattice spacing measured on different areas of the HRTEM micrograph shown in (a)

At a post annealing temperature of 350 °C, a very uniform thin layer of ZnO nanoparticles could be observed (Fig. 7a). Lattice spacing of 0.26 nm measured at different sections of the TEM image of Fig. 8a confirm the existence of a highly oriented crystalline layer with the *c*-axis pointing vertically out of the substrate. Three of the measured areas are shown in Fig. 8b–d. As expected, the ZnO

nanorods grown from this highly oriented seed layer are vertical with almost comparable widths lying between 200 and 300 nm. The top view and the cross-sectional micrograph of the nanorods are shown in Fig. 7b, c.

When the annealing temperature was further increased to 450 °C, ZnO crystallized into nanoparticles as well as nanorod like structures which are visible in the SEM image

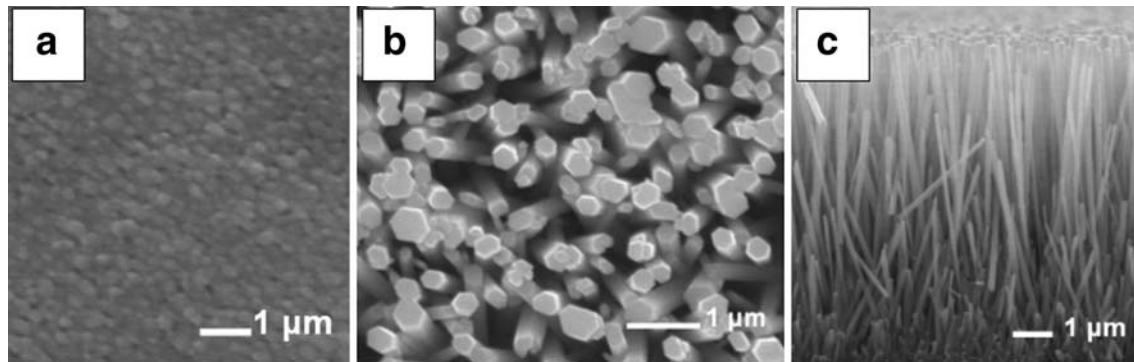


**Fig. 7** **a** ZnO seeds on glass substrate prepared from zinc acetate with a preheating temperature of 120 °C and post annealing at 350 °C for 5 h **b** Scanning electron microscopy (SEM) image of ZnO nanorods grown on substrate **(a)** and **c** cross-sectional view of the vertical nanorods

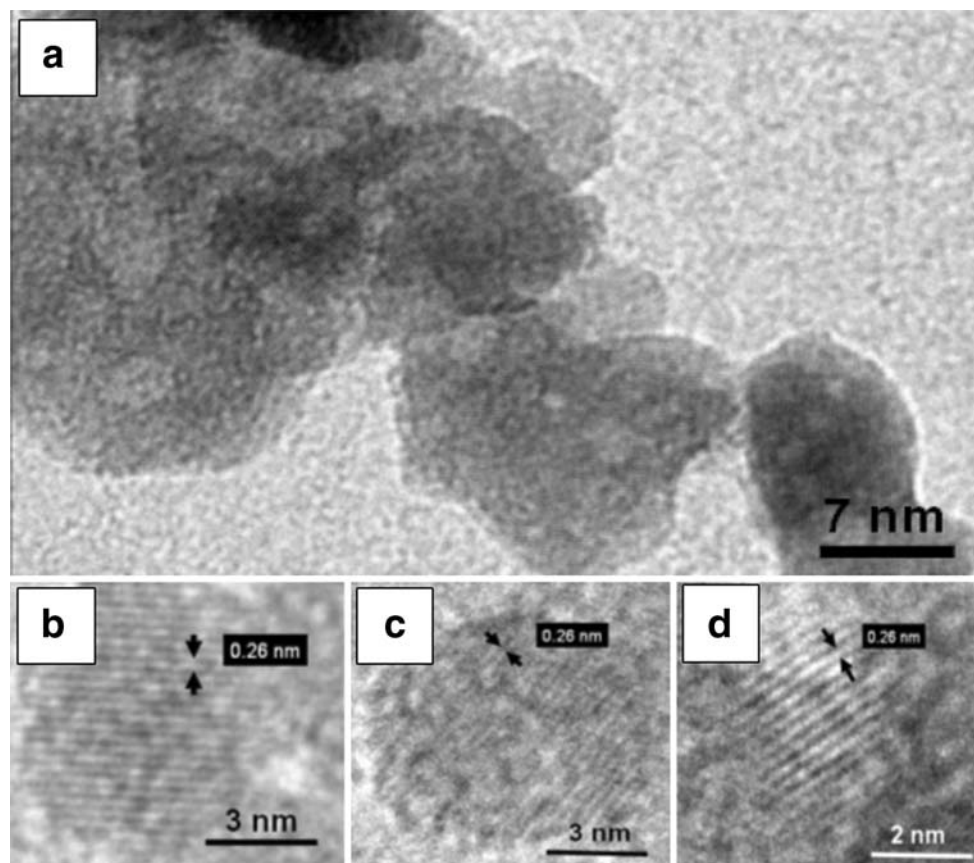


**Fig. 8** **a** Transmission electron microscope (TEM) image of the seeds formed at a preheating temperature of 120 °C and post annealing at 350 °C for 1 h **b**, **c**, **d** Lattice spacing measured on different areas of the HRTEM micrograph shown in **(a)**

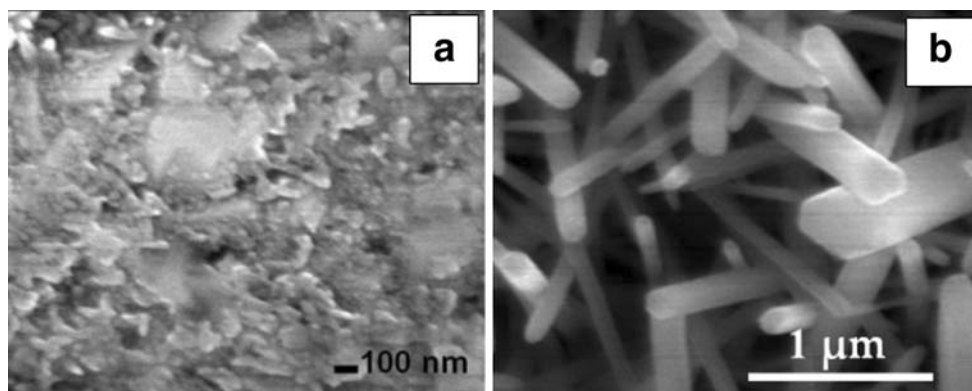


**Fig. 9** **a** Substrate seeded with zinc acetate with preheating at 120 °C and post annealing at 450 °C for 1 h **b** Scanning electron microscope (SEM) image of ZnO nanorods grown on (a) using a 10 mM chemical bath

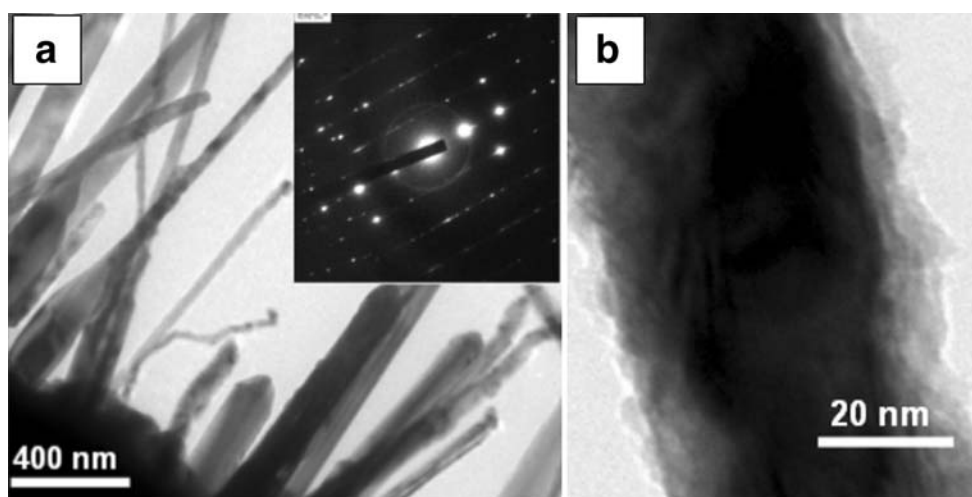


**Fig. 10** **a** Transmission electron microscope (TEM) image of the seeds formed at a preheating temperature of 120 °C and post annealing at 450 °C for 1 h. Inset: Diffraction pattern **(b)** HRTEM micrograph showing a single nanorod

shown in Fig. 9a. Owing to wide variation in sizes of the nucleation seed crystallites, the nanorods grown on such a seeded substrate had widths varying from 50 nm to about 700 nm (Fig. 9b). The nanorods grew without any specific orientation.

The TEM image taken on a similar seed layer grown on a copper grid is shown in Fig. 10a. The ZnO nanorods are longer than those seen in the SEM image in Fig. 9a probably due to the presence of copper in the TEM grid which may have acted as a catalyst aiding the ZnO crystal growth. The diffraction pattern (inset of Fig. 10a) shows the single crystalline nature of the ZnO nanorod like crystals. Figure 10b shows a HRTEM image of a single rod.

As the (001) direction is the fastest growing direction for ZnO crystals, the lengths of the nanorods grown for a specific duration are comparable no matter whether they are grown from nanoparticle seeds or nanocrystalline thin

films. However, the lateral growth is observed to be higher in the case of nanoparticle seeding which can be attributed to the density of the nucleation sites, which is less as compared to in situ growth of nanocrystallites using zinc acetate. From the comparative graphs shown in Fig. 11, it can be observed that even though the growth of the nanorods was done at the same concentration of 10 mM, the growth of the non polar facets contributing to the width of the nanorods was much higher (more than 3 times) when the rods grow out from pre-synthesized ZnO seeds. The nanorods grown on seeds crystallized from zinc acetate solution, therefore, have a higher aspect ratio (of the order of 3) and offer large surface to volume ratio and are ideal for sensors. Figure 12 show SEM micrographs of vertical growth of ZnO nanorods on zinc acetate seeded substrates for different growth durations (5, 8, 10 and 15 h).

**Fig. 11** Comparative growth of ZnO nanorods grown on substrates seeded using ZnO nanoparticles and zinc acetate for a duration of 15 h **a** width **b** length

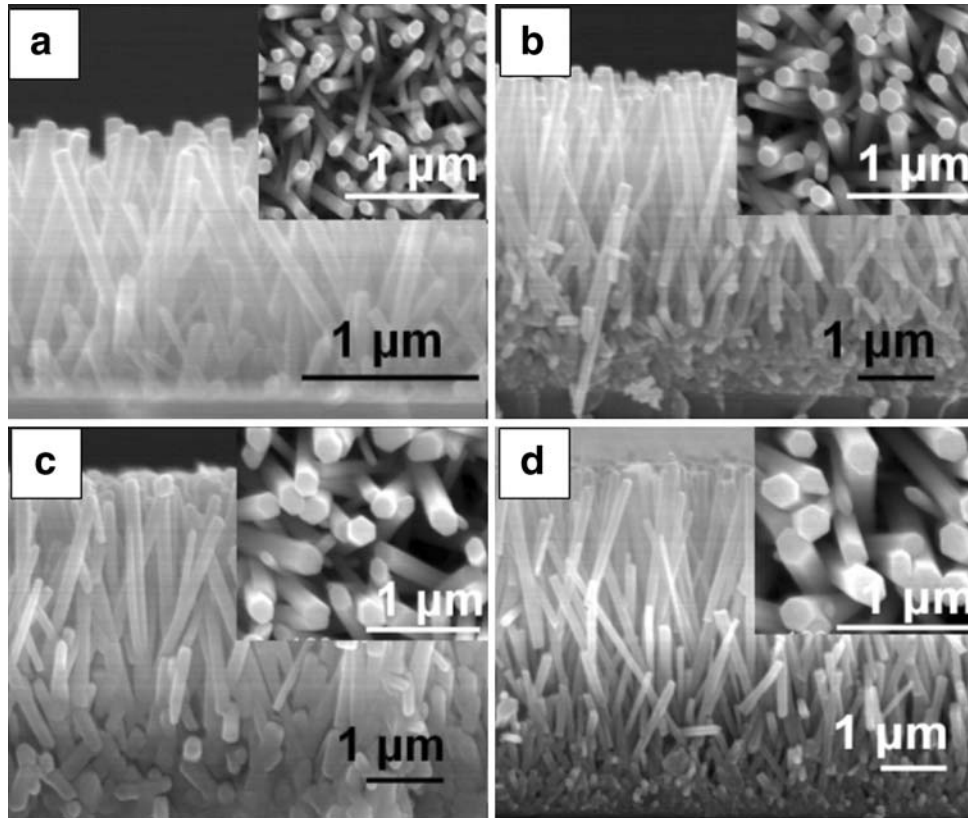
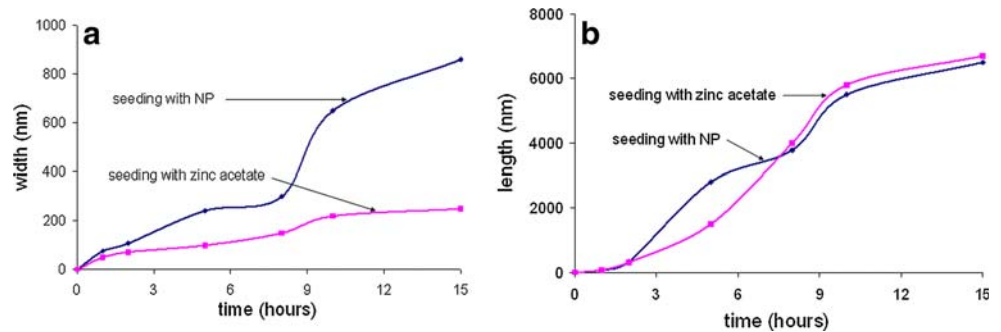


**Fig. 12** Scanning electron microscope (SEM) images of the ZnO nanorods grown in a chemical bath of 10 mM concentration with different growth durations **a** 5 h **b** 8 h **c** 10 h and **d** 15 h. Insets: top views

#### 4 Conclusion

We have successfully grown ZnO nanorods with different orientations to cater to the multifarious applications of ZnO in photonics, piezotronics and filters for the electronic industry. This work highlights the importance of seeding on the growth and orientation of the ZnO nanorods. While seeding with ZnO nanoparticles in colloidal form produced nanorods which were oriented like flowers, seeding with zinc acetate gave different morphology and orientations based upon the preheating and post annealing temperatures used during the growth of the seed layer.

Vertically aligned rods were obtained on substrates seeded using a preheating temperature of 120 °C and a post annealing temperature of 350 °C for 5 h. Aspect ratio of the nanorods grown on zinc acetate seeded substrates was higher than the ones grown from nanoparticles seeded substrates by a factor close to 3.

**Acknowledgments** The authors would like to acknowledge partial financial support from the National Nanotechnology Center, belonging to the National Science & Technology Development Agency (NSTDA), Ministry of Science and Technology (MOST), Thailand and the Centre of Excellence in Nanotechnology at the Asian Institute of Technology, Thailand.



## References

1. Zhang J, Sun L, Pan H, Liao C, Yan C (2002) *N J Chem* 26:33. doi:[10.1039/b108172a](https://doi.org/10.1039/b108172a)
2. Hornyak GL, Dutta J, Tibbals HF, Rao AK (2008) *Introduction to nanoscience*. Taylor & Francis, NY
3. Xu J, Chen Y, Li Y, Shen J (2005) *J Mater Sci* 40:2919. doi:[10.1007/s10853-005-2435-4](https://doi.org/10.1007/s10853-005-2435-4)
4. Hossain MK, Ghosh SC, Boontongkong Y, Thanachayanont C, Dutta J, Metastable Nanocryst J (2005) *Mater* 23:27
5. Law M, Greene LE, Johnson JC, Saykally R, Yang P (2005) *Nature. Mater Lett* 4:455
6. Wang X, Song J, Liu J, Wang ZL (2007) *Science* 316:102. doi:[10.1126/science.1139366](https://doi.org/10.1126/science.1139366)
7. Zhang Y, Yu K, Ouyang S, Zhu Z (2006) *Mater Lett* 60:522. doi:[10.1016/j.matlet.2005.09.028](https://doi.org/10.1016/j.matlet.2005.09.028)
8. Vayssieres L, Keis K, Lindquist SE, Hagfeldt A (2001) *J Phys Chem B* 105:3350. doi:[10.1021/jp010026s](https://doi.org/10.1021/jp010026s)
9. Greene LE, Law M, Goldberger J, Kim F, Johnson JC, Zhang Y, Saykally RJ, Yang P (2003) *Angew Chem Int Ed* 42:3031. doi:[10.1002/anie.200351461](https://doi.org/10.1002/anie.200351461)
10. Sugunan A, Warad HC, Boman M, Dutta J (2006) *J Sol-Gel Sci Technol* 39:49. doi:[10.1007/s10971-006-6969-y](https://doi.org/10.1007/s10971-006-6969-y)
11. Shi G, Mo CM, Cai WL, Zhang LD (2005) *Solid State Commun* 115:253. doi:[10.1016/S0038-1098\(00\)00169-1](https://doi.org/10.1016/S0038-1098(00)00169-1)
12. Baruah S, Thanachayanont C, Dutta J (2008) *Sci Technol Adv Mater* 9:025009. doi:[10.1088/1468-6996/9/2/025009](https://doi.org/10.1088/1468-6996/9/2/025009)
13. Cross RBM, De Souza MM, Narayanan EMS (2005) *Nanotechnology* 16:2188. doi:[10.1088/0957-4484/16/10/035](https://doi.org/10.1088/0957-4484/16/10/035)
14. Bahnemann DW, Kormann C, Hofmann R (1987) *J Phys Chem* 91:3789. doi:[10.1021/j100298a015](https://doi.org/10.1021/j100298a015)
15. Chaudret B (2005) *C R Phys* 6:117. doi:[10.1016/j.crhy.2004.11.008](https://doi.org/10.1016/j.crhy.2004.11.008)
16. Jafri SHM, Sharma AB, Thanachayanont C, Dutta J (2006) *Mater Res Soc Symp Proc* vol 901E
17. Claesson EM, Philippe AP (2007) *Colloids Surf A Physicochem Eng Asp* 297:46. doi:[10.1016/j.colsurfa.2006.10.019](https://doi.org/10.1016/j.colsurfa.2006.10.019)
18. Baruah S, Rafique RF, Dutta J (2008) *Nano* 3:1
19. Dutta J, Hofmann H (2004) *Self Organization of Colloidal Nanoparticles*, *Encyclopedia of Nanoscience & Nanotechnology* 9:617 ed. H. S. Nalwa, American Scientific Publishers, USA
20. Wang M, Zhang L (2009) *Mater Lett* 63:301. doi:[10.1016/j.matlet.2008.10.022](https://doi.org/10.1016/j.matlet.2008.10.022)
21. Santos AMP, Santos EJP (2008) *Thin Solid Films* 516:6210. doi:[10.1016/j.tsf.2007.11.111](https://doi.org/10.1016/j.tsf.2007.11.111)
22. Wei M, Zhi D, MacManus-Driscoll JL (2005) *Nanotechnology* 16:1364. doi:[10.1088/0957-4484/16/8/064](https://doi.org/10.1088/0957-4484/16/8/064)
23. Paraguay FD, Estrada WL, Acosta DRN, Andrade E, Miki-Yoshida M (1999) *M. Thin Solid Films* 350:192. doi:[10.1016/S0040-6090\(99\)00050-4](https://doi.org/10.1016/S0040-6090(99)00050-4)
24. Hocheplid JF, de Oliveira APA, Guyot-Ferreol V, Tranchant JF (2005) *J Cryst Growth* 283:156. doi:[10.1016/j.jcrysgro.2005.05.051](https://doi.org/10.1016/j.jcrysgro.2005.05.051)
25. Lima RC, Macario LR, Espinosa JWM, Longo VM, Erlo R, Marana NL, Sambrano JR, dos Santos ML, Moura AP, Pizani PS, Andrés J, Longo E, Varela JA (2008) *J Phys Chem A* 112:8970. doi:[10.1021/jp8022474](https://doi.org/10.1021/jp8022474)
26. Baruah S, Dutta J (2009) *Sci Technol Adv Mater* 10:013001. doi:[10.1088/1468-6996/10/1/013001](https://doi.org/10.1088/1468-6996/10/1/013001)